

# Standard clinical computed tomography fails to precisely visualise presence, course and branching points of deep cerebral perforators

R. Rzepliński<sup>1</sup>, M. Sługocki<sup>1</sup>, M. Kwiatkowska<sup>2</sup>, S. Tarka<sup>2</sup>, M. Tomaszewski<sup>3</sup>, M. Kucewicz<sup>3</sup>, K. Karczewski<sup>4</sup>, P. Krajewski<sup>2</sup>, J. Małachowski<sup>3</sup>, B. Cizek<sup>1</sup>

<sup>1</sup>Department of Descriptive and Clinical Anatomy, Medical University of Warsaw, Poland

<sup>2</sup>Department of Forensic Medicine, Medical University of Warsaw, Poland

<sup>3</sup>Institute of Mechanics and Computational Engineering, Faculty of Mechanical Engineering, Military University of Technology, Warsaw, Poland

<sup>4</sup>Institute of Materials Science and Engineering, Faculty of Advanced Technologies and Chemistry, Military University of Technology, Warsaw, Poland

[Received: 29 October 2021; Accepted: 28 November 2021; Early publication date: 15 December 2021]

**Background:** Standard computed tomography (CT) images have earned a well-established position in neuroimaging. Despite that, CT is somehow limited by its resolution, which does not enable to distinctively visualise structures smaller than 300 µm in diameter. Perforating arteries, most of which measure 100–400 µm in diameter, supply important subcortical structures (thalamus, basal ganglia, internal capsule). Consequently, pathologies affecting these vessels (e.g. lacunar strokes) can have a devastating clinical outcome. The aim of our study was to assess standard CT's ability to visualise perforators and compare it with microscopic and micro-CT pictures.

**Materials and methods:** We have obtained 6 brainstem and 17 basal ganglia specimens. We infused them with barium sulphate contrast medium administered into either vertebral or internal cerebral artery. After that, the specimens were fixed in formalin and subsequently a series of CT, micro-CT and microscopic examinations were performed.

**Results:** The median number of visualised perforators in brainstem and basal ganglia specimens was 8 and 3, respectively for CT and 18 and 7 for micro-CT ( $p < 0.05$ ). Standard CT failed to clearly visualise branching points and vessels smaller than 0.25–0.5 mm (1–2 voxels) in diameter. Parallel vessels, like lenticulostriate arteries could not be differentiated in standard CT due to their proximity being smaller than the resolution.

**Conclusions:** Basing on our results, we infer that CT is a poor modality for imaging of the perforators, presenting both quantitative and qualitative flaws in contrast with micro-CT. (Folia Morphol 2023; 82, 1: 37–41)

**Key words:** perforating arteries, cerebral perforators, computed tomography, micro-computed tomography, cerebral circulation

Address for correspondence: R. Rzepliński, MD, Department of Descriptive and Clinical Anatomy, Medical University of Warsaw, ul. Chałubińskiego 5, 02–004 Warszawa, Poland, tel/fax: +48 22 629 52 83, e-mail: radoslaw.rzeplinski@wum.edu.pl

This article is available in open access under Creative Common Attribution-Non-Commercial-No Derivatives 4.0 International (CC BY-NC-ND 4.0) license, allowing to download articles and share them with others as long as they credit the authors and the publisher, but without permission to change them in any way or use them commercially.

## INTRODUCTION

The clinical significance of the anatomy of cerebral perforating arteries is well known [14]: despite their relatively small diameter of below 1 mm [3, 5], their pathology results in development of serious diseases such as lacunar stroke, intracerebral haemorrhage, vascular dementia, as well as leads to severe ischaemic complications after aneurysmal subarachnoid haemorrhage and neurovascular procedures [1, 2, 8, 9, 11]. Despite advances in neuroimaging techniques, assessment of presence and function of perforating arteries remains challenging.

The aim of the study was to assess suitability of standard contrast enhanced computed tomography (CT) for visualising deep cerebral perforators by comparing its results to microscopic and micro-computed tomography (micro-CT) studies of anatomical specimens.

## MATERIALS AND METHODS

### Preparation of the specimens

The specimens of basal ganglia and brainstem were prepared by obtaining an unfixed brain from the cadaver, filling the arteries with contrast medium (barium sulphate), and fixing in 10% buffered formalin solution, as precisely described previously [12]. In each case, the pontine branches of the basilar artery (from the vertebrobasilar junction to the superior cerebellar arteries) or the lenticulostriate arteries were counted and measured using a microsurgical microscope.

### Scanning of the specimens and radiological analysis

Every specimen was scanned with both standard clinical CT scanner (Toshiba Asteion TSX-034A, voxel size 0.25 mm, 120 kV, 150 mA) and micro-CT scanner (Nikon Metris XT H 225 ST, voxel size 0.0034 mm, 225 kV, 4 million pixels detector). Images were processed in CT Pro 3D software (Metris XT 2.2, Nikon Metrology, Belmont, CA) and Mimics Innovation Suite 24.0 (Materialise, Belgium). The pontine branches or the lenticulostriate arteries were counted in each case. The quality of visualisation of the branching sites and the course of the arteries were also determined. The numbers of arteries visualised in standard and micro-CT were compared with the Wilcoxon signed rank sum test.

### Ethical approval

All procedures performed in the study were in accordance with the ethical standards of the institutional research committee and with the 1964 Helsinki declaration and its later amendments. The study protocol was approved by The Ethics Committee of Medical University of Warsaw, Poland (Number 138/2020).

## RESULTS

Six specimens of brainstem and 17 specimens of basal ganglia were prepared and scanned by both standard and micro-CT. The median (first–third quartile) number of the pontine branches of the basilar artery amounted to 8 (7–9) and 18 (17–21) in standard and micro-CT, respectively ( $p = 0.031$ ). The median (first–third quartile) number of the lenticulostriate arteries amounted to 3 (3–4) and 7 (7–8) in standard and micro-CT, respectively ( $p < 0.0001$ ). Numbers of arteries counted under microsurgical microscope and visualised in micro-CT were equal in all cases — every artery filled with contrast medium was visible in micro-CT. Diameters of the perforating arteries measured with the use of microsurgical microscope ranged from 0.11 to 0.76 mm and were equal to the diameters measured on micro-CT scans with an accuracy of arterial wall thickness. In standard CT vessels of diameter below 1–2 voxel sizes (0.25–0.5 mm) were either invisible or could not be measured reliably (Fig. 1). Moreover, perforating arteries tend to have parallel course (e.g. lenticulostriate arteries branching from M2 and distal M1 entering the hemisphere in the anterior perforated substance) and standard CT does not allow to differentiate them, because of distance between the arteries being smaller than the resolution. Therefore, counting and measuring perforating arteries in standard CT scans was significantly compromised. In contrast, micro-CT scans provided clear and precise geometry of branching points and course of studied arteries (Figs. 1, 2).

## DISCUSSION

The main purpose of the study was to investigate suitability of standard CT for visualising perforating arteries of cerebral circulation. Our work clearly shows that this method is ineffective and unreliable. There are several quantitative and qualitative differences between standard CT scans on the one hand and microscopic and micro-CT studies on the other.

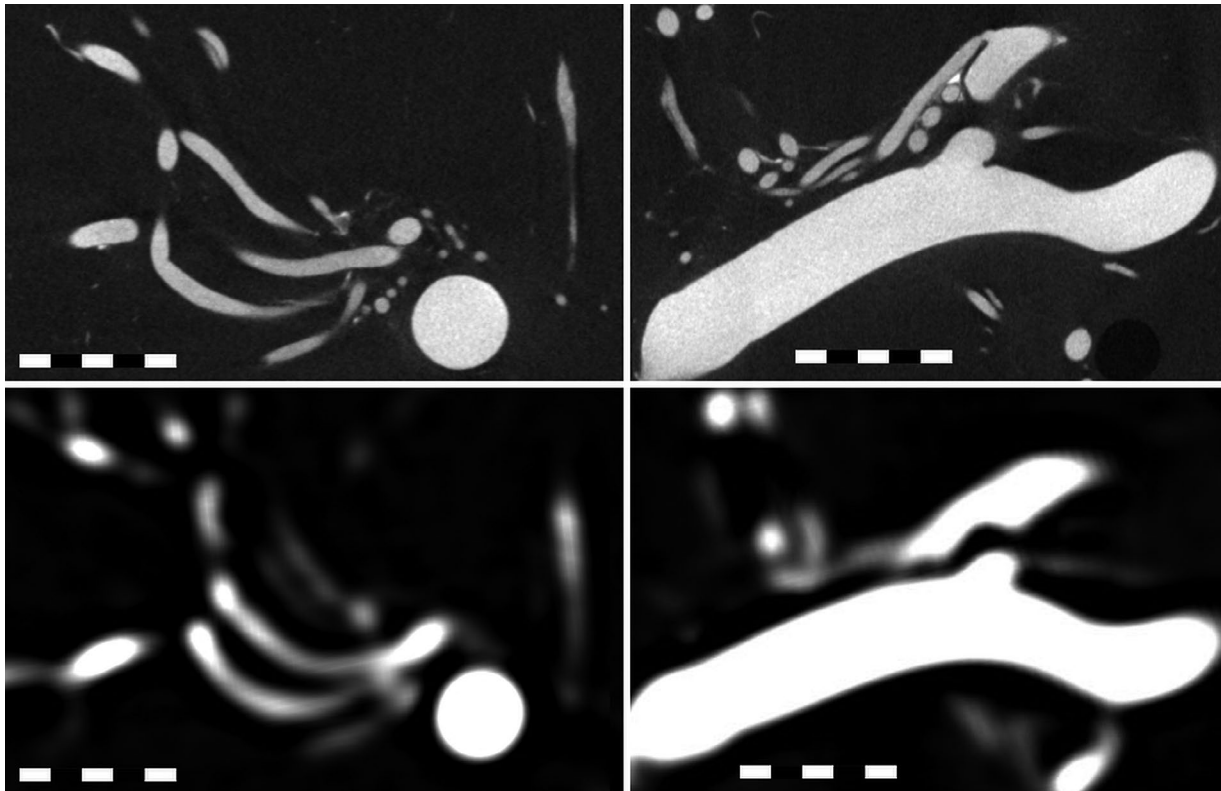


**Figure 1.** Comparison of micro-computed tomography (CT) (upper row) and standard CT (lower row) images in the same plane of a representative middle cerebral artery. Resolution of the standard CT image does not allow to differentiate parallel lenticulostriate arteries and some perforators are invisible. In standard CT a group of perforators can easily be misinterpreted as one vessel. The diameters of the lenticulostriate arteries cannot be measured accurately because the lack of a clear border between contrast-enhanced vessel lumen and non-enhanced surrounding tissues. The branching points cannot be identified in the case of standard CT. Length of the ruler is 5 mm.

#### Quantitative differences between standard and micro-CT scans

The number of visualised pontine and perforating arteries was significantly higher, when counted using microscopic or micro-CT images, which was mainly due to better visualisation of smaller vessels. The resolution of standard CT significantly limited the ability to visualise the perforating arteries, because their diameters usually do not exceed 1–2 sizes of voxel.

Moreover, the number and the diameters of perforators in the micro-CT picture was the same as under the microsurgical microscope, suggesting that these techniques can be utilized interchangeably. This advantage is important especially when studying internal microvasculature as surrounding tissues can be left intact.

#### Qualitative differences between standard and micro-CT scans

As presented above, the standard CT could visualise only the presence of the biggest perforating arteries. What's more interesting, the resolution was not high

enough to study geometry of branching points or courses of the arteries. The micro-CT has visualised branching points and the courses of the perforating arteries far better than the standard CT. Moreover, standard CT scans could not precisely determine the number and branching points of parallel lenticulostriate arteries or pontine branches, making determination of the parent segment impossible. These properties are crucial to plan intracranial procedures, create reliable three-dimensional models, analyse supply areas, dynamics of blood flow and forces acting on arterial walls. Micro-CT allows studying all of the aforementioned aspects.

Noteworthy, angio-CT of the head usually visualises veins to some extent, which further reduces the quality of image. It is especially important in the case of the lenticulostriate arteries because they are located parallel to the deep middle cerebral vein.

The resolution of digital subtraction angiography and magnetic resonance imaging (even 7T [4]) usually do not reach values below 0.25 mm [6, 7]: therefore, one can anticipate the same problems with visualising the perforators as in the case of CT.

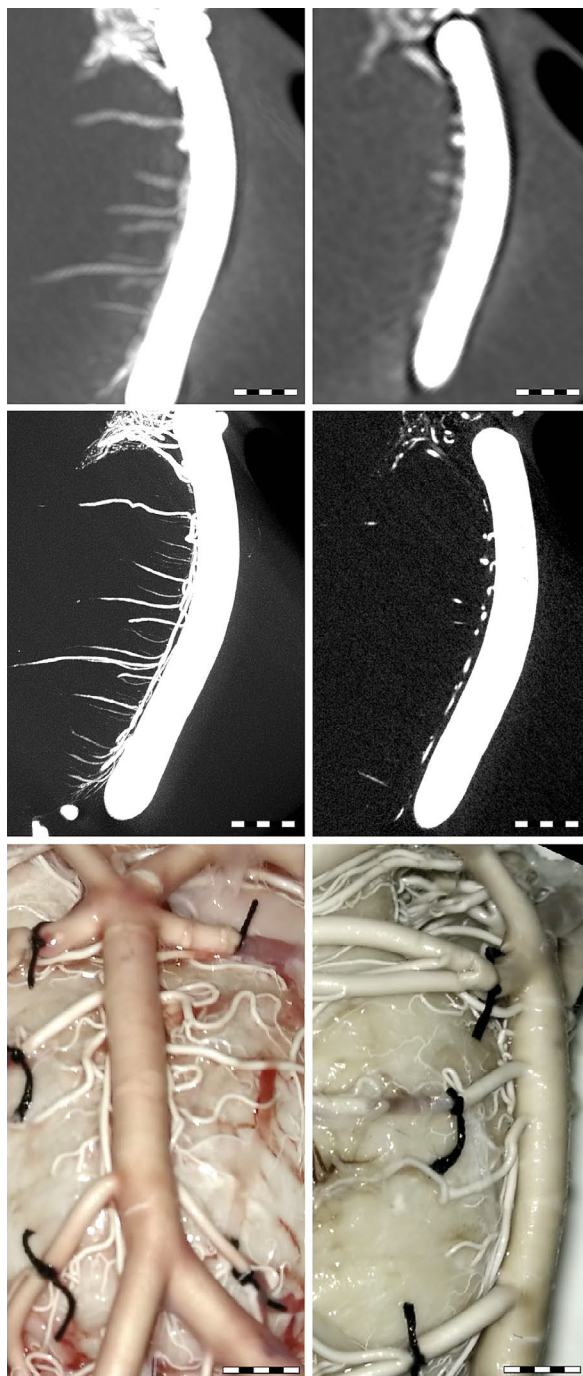


**Figure 2.** Comparison of standard-computed tomography (CT) (top) and micro-CT (middle) images in the same plane and microscopic images of a fixed brainstem specimen (bottom). The CT images on the left side are maximum intensity projection reconstructions (thickness 6.0 mm), and the CT images on the right side are mid-line sagittal slices. Some of the perforating arteries are invisible in standard CT. Similarly, branching points are not evident. Microscopic images show anterior and lateral view of the basilar artery and pontine branches. Length of the ruler is 5 mm.

### Clinical relevance of the study

Our study clearly shows that absence of a structure in imaging studies is not equivalent to non-existence in real life. This conclusion is critical, when studying cerebral vasculature, as the resolution is comparable to the diameters of some arteries (including variants of the circle of Willis with hypoplastic anterior cerebral artery or posterior communicating artery) [10]. Neurosurgeons and neuroradiologists should be aware of that fact when planning and performing intracranial interventions. Micro-CT is a useful tool in preclinical studies [13, 15].

### Limitations of the study

The study was specimen-based; however, standard clinical CT scanner was used. Up to date, no micro-CT scanners are admitted to clinical use. It is only possible to study previously prepared anatomical specimens. The volume of the specimen is usually restricted due to technical features of scanners.

## CONCLUSIONS

Computed tomography is inappropriate to study presence, course, and geometry of the perforating arteries of cerebral circulation. Micro-CT, in contrast, is a feasible and effective method that allows for precise determination of the number, branching points, and the course of the pontine and perforating arteries. These advantages may be used for several anatomical and haemodynamic studies; however, clinical application is restricted by technical features of micro-CT scanners.

### Acknowledgements

The authors sincerely thank those who donated their bodies to science so that anatomical research could be performed. Results from such research can potentially increase mankind's overall knowledge that can then improve patient care. Therefore, these donors and their families deserve our highest gratitude.

### Funding

The study was funded by the National Science Centre, Poland (award number 2020/37/B/ST8/03430, Recipient: Jerzy Małachowski). The National Science Centre had no involvement in the study design, in the

collection, analysis and interpretation of data, in the writing of the manuscript, in the decision to submit the manuscript for publication. Michał Tomaszewski is recipient of Foundation for Polish Science scholarship.

**Conflict of interest:** None declared

## REFERENCES

1. Brinjikji W, Murad MH, Lanzino G, et al. Endovascular treatment of intracranial aneurysms with flow diverters: a meta-analysis. *Stroke*. 2013; 44(2): 442–447, doi: [10.1161/STROKEAHA.112.678151](https://doi.org/10.1161/STROKEAHA.112.678151), indexed in Pubmed: [23321438](https://pubmed.ncbi.nlm.nih.gov/23321438/).
2. Cannistraro RJ, Badi M, Eidelman BH, et al. CNS small vessel disease: A clinical review. *Neurology*. 2019; 92(24): 1146–1156, doi: [10.1212/WNL.0000000000007654](https://doi.org/10.1212/WNL.0000000000007654), indexed in Pubmed: [31142635](https://pubmed.ncbi.nlm.nih.gov/31142635/).
3. Ciszek B, Aleksandrowicz R, Zabek M, et al. Classification, topography and morphometry of the early branches of the middle cerebral artery. *Folia Morphol*. 1996; 55(4): 229–230, indexed in Pubmed: [9243859](https://pubmed.ncbi.nlm.nih.gov/9243859/).
4. Hartevelde AA, De Cocker LJJ, Dieleman N, et al. High-resolution postcontrast time-of-flight MR angiography of intracranial perforators at 7.0 Tesla. *PLoS One*. 2015; 10(3): e0121051, doi: [10.1371/journal.pone.0121051](https://doi.org/10.1371/journal.pone.0121051), indexed in Pubmed: [25774881](https://pubmed.ncbi.nlm.nih.gov/25774881/).
5. Kwiatkowska M, Ciszek B. The anatomy of the median branches of the basilar artery. *Folia Morphol*. 2000; 59(4): 323–325, indexed in Pubmed: [11107706](https://pubmed.ncbi.nlm.nih.gov/11107706/).
6. Naidich TP. (ed). *Imaging of the brain*. Saunders/Elsevier, Philadelphia 2013.
7. Osborn AG, Hedlund GL, Salzman KL. *Osborn's brain: imaging, pathology, and anatomy*. 2 ed. Elsevier, Philadelphia 2018.
8. Phillips TJ, Wenderoth JD, Phatouros CC, et al. Safety of the pipeline embolization device in treatment of posterior circulation aneurysms. *AJNR Am J Neuroradiol*. 2012; 33(7): 1225–1231, doi: [10.3174/ajnr.A3166](https://doi.org/10.3174/ajnr.A3166), indexed in Pubmed: [22678845](https://pubmed.ncbi.nlm.nih.gov/22678845/).
9. Regenhardt RW, Das AS, Lo EH, et al. Advances in understanding the pathophysiology of lacunar stroke: a review. *JAMA Neurol*. 2018; 75(10): 1273–1281, doi: [10.1001/jamaneurol.2018.1073](https://doi.org/10.1001/jamaneurol.2018.1073), indexed in Pubmed: [30167649](https://pubmed.ncbi.nlm.nih.gov/30167649/).
10. Rhoton A. The supratentorial arteries. *Neurosurgery*. 2002; 51(suppl\_4): S1-53-S1-120, doi: [10.1097/00006123-200210001-00003](https://doi.org/10.1097/00006123-200210001-00003).
11. Rzepliński R, Kostyra K, Skadorwa T, et al. Acute platelet response to aneurysmal subarachnoid hemorrhage depends on severity and distribution of bleeding: an observational cohort study. *Neurosurg Rev*. 2021; 44(5): 2647–2658, doi: [10.1007/s10143-020-01444-7](https://doi.org/10.1007/s10143-020-01444-7), indexed in Pubmed: [33241455](https://pubmed.ncbi.nlm.nih.gov/33241455/).
12. Rzepliński R, Tomaszewski M, Stugocki M, et al. Method of creating 3D models of small caliber cerebral arteries basing on anatomical specimens. *J Biomech*. 2021; 125: 110590, doi: [10.1016/j.jbiomech.2021.110590](https://doi.org/10.1016/j.jbiomech.2021.110590), indexed in Pubmed: [34214861](https://pubmed.ncbi.nlm.nih.gov/34214861/).
13. Skadorwa T, Maślanka M, Ciszek B. The morphology and morphometry of the fetal fallopian canal: a microtomographic study. *Surg Radiol Anat*. 2015; 37(6): 677–684, doi: [10.1007/s00276-014-1395-2](https://doi.org/10.1007/s00276-014-1395-2), indexed in Pubmed: [25480106](https://pubmed.ncbi.nlm.nih.gov/25480106/).
14. Vogels V, Dammers R, van Bilsen M, et al. Deep cerebral perforators: anatomical distribution and clinical symptoms: an overview. *Stroke*. 2021; 52(10): e660–e674, doi: [10.1161/STROKEAHA.120.034096](https://doi.org/10.1161/STROKEAHA.120.034096), indexed in Pubmed: [34311568](https://pubmed.ncbi.nlm.nih.gov/34311568/).
15. Wojciechowski T, Skadorwa T, Nève de Mévergnes JG, et al. Microtomographic morphometry of the stapedius muscle and its tendon. *Anat Sci Int*. 2020; 95(1): 31–37, doi: [10.1007/s12565-019-00490-6](https://doi.org/10.1007/s12565-019-00490-6), indexed in Pubmed: [31111392](https://pubmed.ncbi.nlm.nih.gov/31111392/).